

A new porphyrin sensitizer with phenolic binding group for high efficiency dye-sensitized solar cells

LIGUO JIN¹, HONGJIE WANG¹, SHUO WANG¹, LIPING WEN⁴, JIN ZHAI^{*2}, TIANXIN WEI³

¹The School of Material Science & Engineering, Harbin University of Science and Technology, Harbin 150040, P. R. China

²Key Laboratory of Bio-Inspired Smart Interfacial Science and Technology of Ministry of Education, School of Chemistry and Environment, Beihang University, Beijing 100191, P. R. China

³Institute for Chemical Physics, Beijing Institute of Technology, Beijing, 100081, P. R. China

⁴Institute of Chemistry, Chinese Academy of Sciences, Beijing 100190, P. R. China

A novel zinc porphyrin (5,10,15-tri-dodecoxyphenyl-20-(4-hydroxyphenyl-azo-benzenyl)-porphyrinatozinc (tdhab-ZnP)) with benzenyl-azo-phenolic group, able to adsorb on the nanocrystalline-TiO₂ film, has been synthesized. We constructed a dye-sensitized solar cell based on the nanocrystalline-TiO₂ hierarchical structure film, with a power conversion efficiency of 4.15 % and a high current density of 14 mA/cm² under AM 1.5 irradiation. UV-Vis absorption spectra measurements indicated that the tdhab-ZnP molecules formed a charge transfer complex with TiO₂ nanoparticles (NPs) through the phenolic group. Cyclic voltammetry measurement showed that the charge separation resulting from the tdhab-ZnP excited singlet state to the conduction band (CB) of TiO₂ and charge shifting from the I⁻/I₃⁻ couple to the porphyrin radical cation were thermodynamically feasible.

Keywords: *dye-sensitized solar cell; porphyrin; nanocrystalline-TiO₂*

© Wrocław University of Technology.

1. Introduction

Dye-sensitized solar cells (DSSCs) based on nanocrystalline semiconductors have received considerable attention because of their relatively low cost and high efficiency for the photo-electrical conversion of solar energy [1, 2]. Sensitizers, as a key components in DSSCs, exert significant influence on the photovoltaic performance. Ruthenium (II) polypyridyl and its derivatives have so far been regarded as the best sensitizing dyes for solar energy conversion due to their strong visible absorption bands, long-lived excited state and excellent photochemical stability. DSSCs based on Ru dyes can produce solar energy to electricity conversion efficiency (η) of up to 11 % under AM 1.5 irradiation [3–5]. However, these complexes, which show poor red/near-infrared (NIR) light absorption, are unsatisfactory and cause environmental problems. In view of the excellent photochemical and

electrochemical properties of porphyrins and their low cost of production as well as broad absorption in the visible and NIR region, many researchers have taken keen interest in solar cells based on porphyrins dye-sensitized nanocrystalline TiO₂ [6, 7].

In this regard, in the solar cells developed from porphyrin dyes, majority of the anchoring groups are carboxylates [8, 9] and sometimes phosphonates [10] and sulfonates [11]. However, there are some disadvantages in using carboxylate functionality as anchoring groups though they show outstanding photoelectric properties. The ground-state pK_a values of the carboxylates are too low to ensure strong binding [12]. In addition, in the presence of water, slow desorption of the photosensitizers can occur, which may limit the long-term stability of the cell. The aggregation of porphyrin dye, which causes intermolecular energy transfer, is also considered to be one of the factors decreasing photovoltaic performance of DSSCs based on organic dyes [13]. Das et al. [14] have observed that

*E-mail: zhajjin@buaa.edu.cn

catechol binding is stronger than any other type of binding, which can form a charge transfer (CT) complex with TiO_2 NPs through the catechol moiety of porphyrins by a five-membered ring. Campbell et al. [15, 16] have demonstrated that the presence of a conjugated linkage between porphyrin and a binding group significantly enhanced solar cell performance. Recently, it was found that an efficient retardation of the charge recombination process and a significant improvement of device performance could be achieved by using organic dyes with lateral alkyl chains [17, 18]. With the long alkyl chains, the lifetime of electrons can be increased by preventing the acceptors (i.e. I_3^- ion) to approach the TiO_2 surface and/or by reducing the reorganization energy of the dye, resulting in the desired condition for the kinetic competition for reduction of the dye cations [19]. The aggregation of dye molecules would also be suppressed by the steric hindrance due to the long alkyl chains. Up to now, porphyrin sensitizers with carboxylate binding groups have provided a higher photoelectric conversion efficiency than that of other binding groups. In 2010 and 2011, Michael Grätzel's group reported the DSSCs with the novel porphyrin sensitizers that gave an overall conversion efficiency of 11 % and 12 %, which were the best for porphyrin-based sensitizers [20, 21].

Taking these points into account, further development of strategic molecular design of a porphyrin dye is required to achieve higher light-electricity conversion efficiency values. Herein, our design toward the high photovoltaic performance of porphyrin-dye sensitized solar cells is based on the interfacial engineering of a dye adsorbed on TiO_2 surface, which can be controlled by the structural modification of the porphyrin molecule to diminish the charge recombination between the electrons and acceptors, that is, to prevent the recombination of dye cation and I_3^- ions, and the aggregation of the dye molecules.

A π -elongated porphyrin with benzenyl-azophenol was synthesized with phenolic group acting as the bonding group (Fig. 1). The π -elongated porphyrin with azobenzenyl group should benefit from the fast electron injection into the CB of

the semiconductor and slow charge recombination between the injected electron and the sibling dye cation, while introduction of alkyl chain groups ($\text{C}_{12}\text{H}_{25}-$) is expected to enhance the distance between the core of porphyrins and I_3^- ions so that to decrease the dark current, leading to the improvement of the photovoltaic properties.

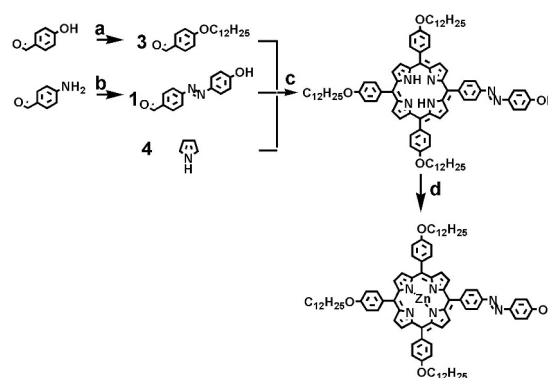


Fig. 1. Reagents and conditions: (a) acetone, $\text{BrC}_{12}\text{H}_{25}$, K_2CO_3 , reflux, N_2 , RT (10 h); (b) HCl , NaNO_2 , 0 to 5 °C; phenol, 0 °C, RT (2 h); (c) CHCl_3 , BF_3OEt_2 , RT (1 h); DDQ; Et_3N , RT (1 h); (d) $\text{Zn}(\text{CH}_3\text{COO})_2$, CH_3OH 70 °C, RT (30 min).

2. Experimental

2.1. Synthesis and characterization

The synthetic route to prepare the porphyrin antenna molecule of (5,10,15-tri-dodecoxyphenyl-20-(4-hydroxyphenyl-azo-benzenyl)-porphyrin (tdhab- H_2P) is shown in Fig. 1. H_2P was prepared by the reaction of p-dodecoxybenzaldehyde, aldehyde-azo-Ph-OH and pyrrole in chloroform under nitrogen atmosphere, at room temperature, under stirring. Five minutes later, boron trifluoride etherate (BF_3OEt_2) was added into the above mixture. After an hour, the proper 2,3-dichloro-5,6-dicyano-1,4-benzoquinone (DDQ) was added to the flask and reacted for 1 hour. Triethylamine (Et_3N) was then used to neutralize the reaction. The mixture solvent was removed and the product was purified using column chromatography (eluent dichloromethane), yielding a purple solid. ^1H NMR (CDCl_3 , 400 MHz): δ = 8.89 (m, broad, 8H, β -pyrrole), 8.35 (d, 2H, $\text{CH}_{\text{ortho-Ph-OH}}$, J = 7.6 Hz), 8.26 (d, 2H, $\text{CH}_{\text{meta-Ph-OH}}$, J = 7.6 Hz),

8.11 (d, 6H, $CH_{ortho-Ph-OC_{12}H_{25}}$, $J = 8.4$ Hz), 8.00 (d, 2H, $CH_{meta-Ph-N=N}$, $J = 8.3$ Hz), 7.26 (d, 6H, $CH_{meta-Ph-OC_{12}H_{25}}$, $J = 7.2$ Hz), 6.89 (d, 2H, $CH_{ortho-Ph-N=N}$, $J = 8.3$ Hz), 4.28 (t, 6H, $OCH_2C_{11}H_{23}$, $J = 6.2$ Hz), 2.33 (s, 1H, Ph-OH), 1.97 (m, 6H, $OCH_2CH_2C_{10}H_{21}$), 1.81 (m, 6H, $OC_2H_4CH_2C_9H_{19}$), 1.62 (m, 6H, $OC_3H_6CH_2C_8H_{17}$), 1.39 (m, 42H, $OC_3H_6C_7H_{14}CH_3$), 0.90 (m, 9H, $OC_{11}H_{22}CH_3$), -2.72 (s, broad, 2H, NH-porphyrin). MS (MALDI-TOF): m/z 1287.7, calculated for $C_{86}H_{106}N_6O_4$:1286.8.

Then tdkhab-ZnP was also prepared from H_2P by Zn(II)-metallation (Fig. 1). 1H NMR ($CDCl_3$, 400 MHz): $\delta = 8.88$ (m, broad, 8H, β -pyrrole), 8.35 (d, 2H, $CH_{ortho-Ph-OH}$, $J = 7.6$ Hz), 8.28 (d, 2H, $CH_{meta-Ph-OH}$, $J = 7.6$ Hz), 8.11 (d, 6H, $CH_{ortho-Ph-OC_{12}H_{25}}$, $J = 7.2$ Hz), 8.00 (d, 2H, $CH_{meta-Ph-N=N}$, $J = 8.3$ Hz), 7.26 (d, 6H, $CH_{meta-Ph-OC_{12}H_{25}}$, $J = 7.2$ Hz), 7.01 (d, 2H, $CH_{ortho-Ph-N=N}$, $J = 8.3$ Hz), 4.26 (t, 6H, $OCH_2C_{11}H_{23}$, $J = 6.2$ Hz), 2.31 (s, 1H, Ph-OH), 2.00 (m, 6H, $OCH_2CH_2C_{10}H_{21}$), 1.81 (m, 6H, $OC_2H_4CH_2C_9H_{19}$), 1.61 (m, 6H, $OC_3H_6CH_2C_8H_{17}$), 1.30 (m, 42H, $OC_3H_6C_7H_{14}CH_3$), 0.89 (m, 9H, $OC_{11}H_{22}CH_3$). MS (MALDI-TOF): m/z 1349.4, calculated for $C_{86}H_{104}N_6O_4Zn$:1348.7.

2.2. Photoelectrochemical solar cells

DSSCs were fabricated as previously described in [22, 23]. Nanocrystalline- TiO_2 hierarchical structure film electrode was fabricated by the electro-hydrodynamic technique (EHD). The TiO_2 colloidal suspension was composed of ethanol (5 mL), polyvinyl alcohol (PVA, MW = 22,000) water solution (1 g, 33 wt.%), titanium sol (6.6 mL, $0.1\text{ g}\cdot\text{L}^{-1}$). Anatase TiO_2 nanoparticles were hydrothermally synthesized according to [24]. The suspension was sprayed onto the conductive fluorine-doped tin oxide (FTO) glass slides (Nippon, $14\ \Omega/\square$) with a buffer layer (the preparation method, of which was described in [22]). Then, the TiO_2 composite film was annealed at $450\ ^\circ\text{C}$ for 1 hour in air, resulting in a $6\ \mu\text{m}$ thick film. The as-prepared

electrode was put into 0.2 M $TiCl_4$ aqueous solution overnight at room temperature and annealed again for 30 min at $450\ ^\circ\text{C}$ in air. The sensitizer was adsorbed onto this film by dipping it into a 0.3 mM tdkhab-ZnP solution dissolved in CH_2Cl_2 and leaving it there overnight. After completion of the dye coating, the electrode was rinsed with dry CH_2Cl_2 and dried in a flow of nitrogen. The DSSC was composed of a sensitized photo-anode, a platinum counter electrode, and an electrolyte. Liquid electrolyte was composed of 0.1 M LiI (Aldrich), 0.05 M iodine (Inland), 0.45 M N-methyl-benzimidazole (NMBI) (Aldrich) and 0.6 M 1-propyl-3-methylimidazolium iodide (MPII) (Shanghai Cheng Jie Chemical Co. Ltd.) in acetonitrile.

2.3. Measurements

The surface morphology and thickness of these porous films were determined by scanning electron microscope (SEM, JEOL, JSM-6700F). The I-V characteristics of the devices were measured using an electrochemical analyzer (CHI630B, Chenhua Instruments Co., Shanghai) under illumination of different simulated solar light intensities (CMH-250, Aodite Photoelectronic Technology Ltd., Beijing) at room temperature. The incident photon-to-current efficiency (IPCE) curve of the DSSCs was measured by illumination with mono-chromatic light, which was obtained by passing light through a series of light filters with different wavelengths. The active area of the solar cell was 0.20 cm^2 . All of the experimental values were given as an average from four independent measurements. The UV-Vis spectra were measured with a spectrophotometer (U-3010, HITACHI). Cyclic voltammetric experiments were performed in 0.03 mM tdkhab-ZnP in CH_2Cl_2 solution at a scan rate of 20 mV/s using 0.1 M tetrabutyl ammonium hexafluorophosphate ($TBAPF_6$) as supporting electrolyte. The working electrode was the FTO glass slide and the saturated calomel electrode (SCE) and platinum foil were the reference electrode and auxiliary electrode, respectively.

3. Results and discussion

3.1. Absorption spectra

Fig. 2 displays UV-Vis spectra and emission spectra of tdhab-ZnP in CH_2Cl_2 solution and on TiO_2 film. The absorption spectrum of tdhab-ZnP in CH_2Cl_2 solution shows a series of visible bands between 400 and 650 nm due to $\pi-\pi^*$ absorptions of the conjugated macrocycle [15]. The tdhab-ZnP (Fig. 2a) exhibits an intense Soret absorption band at 427 nm and two low intensity Q-bands at 552 and 596 nm, respectively. Light absorbing intensity of the Soret absorption band is above 20 times higher of that of Q-bands. Fig. 2b shows the absorption spectrum of tdhab-ZnP adsorbed on TiO_2 nanoparticles. It is interesting to observe that the Soret band of tdhab-ZnP has not changed much for NPs TiO_2 film, however, there is an increment of optical absorption in the broad 400 to 600 nm region. The absorption spectrum of the Q-band of tdhab-ZnP becomes broad and shifted to longer wavelength with an increase in absorbance for the Q-band absorbing at 567 nm and 614 nm, respectively. The corresponding red shift of ~ 15 nm and ~ 18 nm as well as broadening of the Q-band of tdhab-ZnP on TiO_2 NPs, comparing to that of tdhab-ZnP in CH_2Cl_2 solution, can be attributed to the formation of CT complex. It is clear to see that light absorbing intensity of Q-band increases much more comparing to porphyrin in CH_2Cl_2 solution, by above nearly 0.9 times of that of Soret absorption band.

As the tdhab-ZnP molecule binds through the phenol spacer in this case, there may be pure charge transfer (CT) transition due to phenol/ TiO_2 , as shown in Fig. 3. It was reported that TiO_2 NPs can form a strong CT complex with dye molecules, such as alizarin [25], triphenylmethane dyes [26], and Ru-Cat through the catechol spacer. It has already been discussed by Moser et al. [27] that TiO_2 NPs can form a strong complex with catechols by formation of a five-membered ring. Similarly, in the present investigation tdhab-ZnP interacted strongly with TiO_2 NPs by forming CT complex due to the interaction between phenol moiety and TiO_2 NPs, which led to the red shift and the broadening of the Q bands for tdhab-ZnP on TiO_2 NPs.

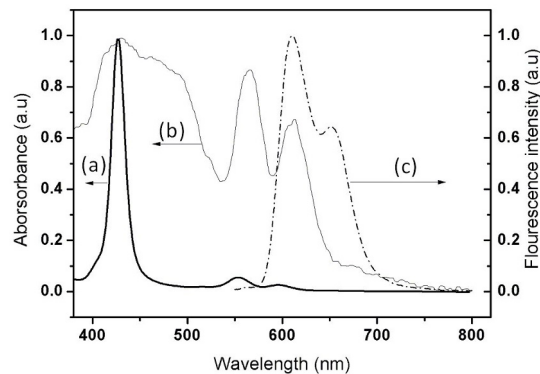


Fig. 2. Normalized absorption spectra of porphyrin: (a) tdhab-ZnP in CH_2Cl_2 solution (thick line); (b) tdhab-ZnP adsorbed onto a TiO_2 film with the thickness of $6 \mu\text{m}$ (thin line); (c) Emission spectrum of tdhab-ZnP in CH_2Cl_2 solution, $\lambda_{ex} = 429$ nm.

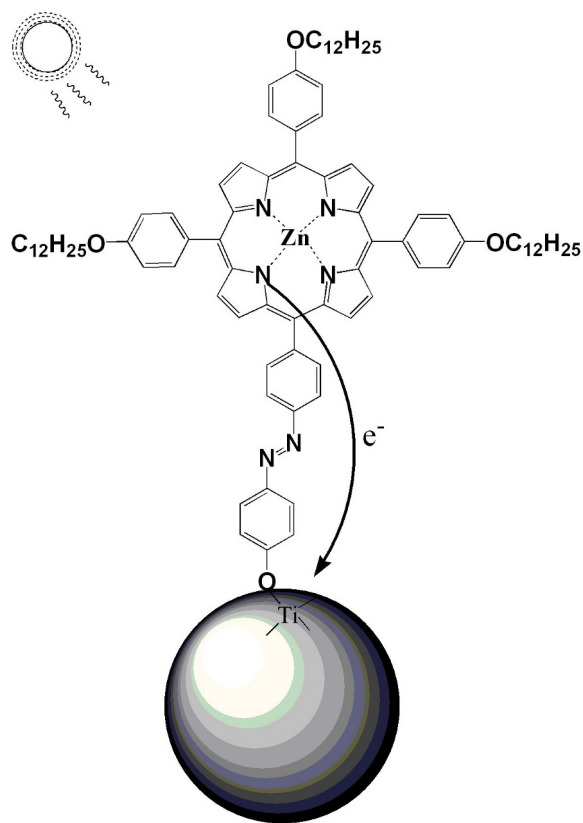


Fig. 3. Molecular structure of tdhab-ZnP and schematic illustration of the complexation reaction between the TiO_2 surface and tdhab-ZnP through phenolic type binding.

3.2. Photovoltaic performance

The current-voltage characteristics were measured using the 6 μm thick TiO_2 films modified with tdhab-ZnP and a Pt counter electrode under different light intensity irradiations. From Fig. 4 and Table 1, the short-circuit photocurrent density (J_{sc}), open-circuit photovoltage (V_{oc}) and fill factor (ff) of tdhab-ZnP sensitized solar cell with liquid electrolyte, measured under the 100 mW/cm^2 light intensity irradiation, are 14.1 mA/cm^2 , 0.521 V and 0.564 , respectively, yielding an overall conversion efficiency (η) of 4.15% , which gives the high photovoltaic performance. We can clearly see that the values of J_{sc} are directly proportional to the light intensity, but the values of η enhance with the light intensity decreasing. The higher photoelectrical conversion efficiency at low light intensity can be ascribed to the higher fill factor (the value varies from 0.565 to 0.686 between 1 and 0.25 sun).

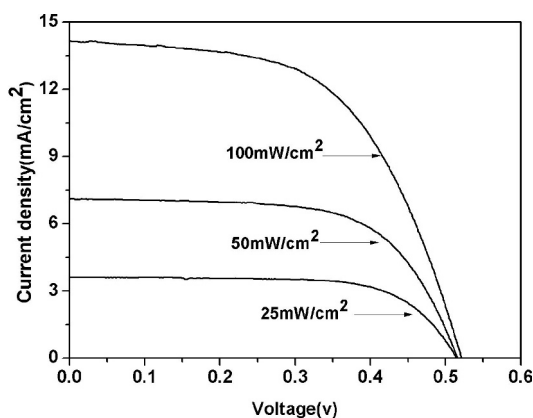


Fig. 4. Photocurrent-voltage plots of tdhab-ZnP-sensitized solar cells measured in liquid electrolyte under illumination of different simulated solar light intensities. The cell active area was 0.2 cm^2 .

Table 1. Device performances of DSSCs with tdhab-ZnP sensitized electrode and liquid electrolyte.

light intensity	J_{sc} (mA/cm ²)	V_{oc} (V)	ff	η
100 mW/cm^2	14.1	0.521	0.565	4.15 %
50 mW/cm^2	7.05	0.515	0.643	4.67%
25 mW/cm^2	3.61	0.514	0.686	5.09%

An action spectrum of IPCE for the tdhab-ZnP-sensitized solar cell is depicted in Fig. 5. It is noteworthy that the tdhab-ZnP-sensitized cell reveals high IPCE values of up to 78% at around 430 nm , extending the response of the photocurrent generation close to 800 nm . The form of the action spectrum of IPCE is similar to that of the absorption spectrum of the tdhab-ZnP adsorbed onto TiO_2 film, which indicates that the tdhab-ZnP displays the excellent photoelectric properties.

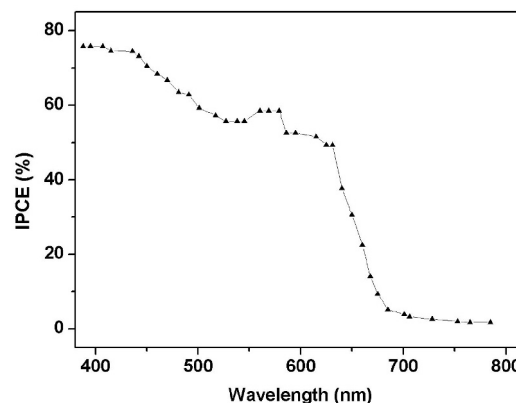


Fig. 5. Photocurrent action spectra of tdhab-ZnP-sensitized solar cells measured with liquid electrolyte.

3.3. Electrochemical properties

Herein, we also discuss the energy level of highest occupied molecular orbital (HOMO) and lower unoccupied molecular orbital (LUMO) of tdhab-ZnP molecule. From the intersection of the normalized absorption and emission spectra in CH_2Cl_2 solution (Fig. 2a and 2c), the zeroth-zeroth energy (E_{0-0}) is determined. The E_{0-0} value of tdhab-ZnP (2.16 eV) implies the HOMO-LUMO gap of the π -elongated porphyrin. Cyclic voltammetry was used to determine the first oxidation potential of tdhab-ZnP. As the result of the cyclic voltammetry measurement (Fig. 6) the first oxidation potential of ZnP was determined as 0.82 V (*vs.* SCE). The energy level of the porphyrin excited singlet state for tdhab-ZnP is -1.34 V (*vs.* SCE) and it is higher than the CB of TiO_2 (-0.74 V *vs.* SCE), [3, 29] whereas the energy level of the porphyrin radical cation for tdhab-ZnP (0.82 V *vs.* SCE) is lower

than those of the I^-/I_3^- couple (0.26 V vs. SCE) (as shown in Fig. 7). Thus, charge separation from the tdhab-ZnP excited singlet state to the CB of TiO_2 and charge shift from the I^-/I_3^- couple to the porphyrin radical cation are thermodynamically feasible.

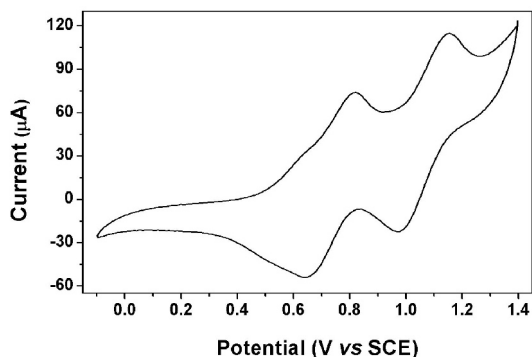


Fig. 6. Cyclic voltammograms of tdhab-ZnP in CH_2Cl_2 containing 0.1 M $TBAPF_6$ as supporting electrolyte. Potentials (V) are given versus SCE (+0.24 V vs. NHE).

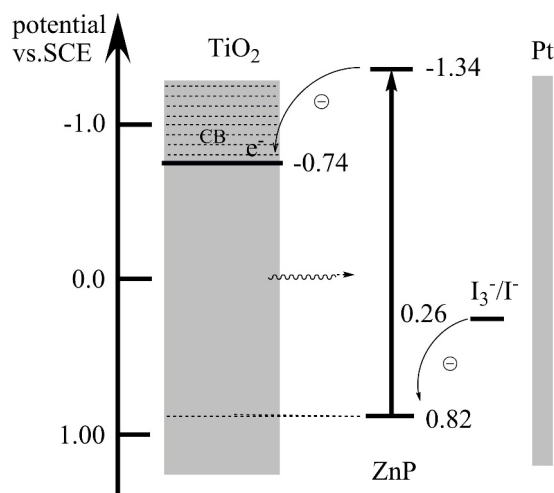


Fig. 7. Mechanistic scheme showing electronic excitation and transfer processes in the ZnP-sensitized nanoparticles TiO_2 solar cell.

4. Conclusions

We have successfully synthesized a novel π -elongated zinc porphyrin with benzenyl-azo-phenol. The zinc porphyrin has been adsorbed

on nanoparticle TiO_2 film by its phenolic group. UV-Vis absorption measurements have indicated that the tdhab-ZnP molecule forms a CT complex with TiO_2 nanoparticles through the phenol moiety, which gives a broad absorption in the visible and NIR regions caused by an interfacial CT transition from the HOMO of tdhab-ZnP to the TiO_2 CB. We constructed a novel photovoltaic cell based on the interfacial CT transition, with a power conversion efficiency of 4.15 % and a high current density of 14.1 mA/cm^2 under AM 1.5 irradiation. These results clearly show that the elongation of a porphyrin π -system with benzenyl-azo-phenol is a useful tactic for collecting solar light in the visible and near infrared regions leading to improved cell performance of porphyrin sensitized solar cells. Further improvement of the power conversion efficiency in porphyrin-sensitized TiO_2 cells will be possible by designing a porphyrin, in which a phenol moiety will be used as the bonding group of porphyrin.

Acknowledgements

We appreciate the financial support of the National Natural Science Foundation of China, the National Research Fund for Fundamental Key Projects (21273060), the Hei-LongJiang Natural Science Fund (15008002-12111) and the HeiLongJiang Postdoctoral Science Fund (LBH-Z12218).

References

- [1] OREGAN B., GRATZEL M., *Nature*, 353 (1991), 737.
- [2] GRATZEL M., *Inorg. Chem.*, 44 (2005), 6841.
- [3] KALYANASUNDARAM K., GRATZEL M., *Coordin. Chem. Rev.*, 177 (1998), 347.
- [4] CLIFFORD J.N., PALOMARES E., NAZEERUDDIN M.K., GRATZEL M., NELSON J., LI X., LONG N.J., DURRANT J.R., *J. Am. Chem. Soc.*, 126 (2004), 5225.
- [5] NAZEERUDDIN MD.K., PÉCHY P., GRÄTZEL M., *Chem. Commun.*, 18 (1997), 1705.
- [6] SHI C.N., ANSON F.C., *Inorg. Chem.*, 35 (1996), 7928.
- [7] CAMPBELL W.M., BURRELL A.K., OFFICER D.L., JOLLEY K.W., *Coordin. Chem. Rev.*, 248 (2004), 1363.
- [8] TRACHIBANA Y., HAQUE S.A., MERCER I.P., DURRANT J.R., KLUG D.R., *J. Phys. Chem. B*, 104 (2000), 1198.
- [9] MONTALTI M., WADHWA S., KIM W.Y., KIPP R.A., SCHMEHL R.H., *Inorg. Chem.*, 39 (2000), 76.
- [10] ODOBEL F., BLART E., LAGREE M., VILLIERAS M., BOUJTITA H., EL MURR N., CARAMORI S., BIGNOZZI C.A., *J. Mater. Chem.*, 13 (2003), 502.
- [11] YANG X.J., DAI Z.F., MIURA A., TAMAI N., *Chem. Phys. Lett.*, 334 (2001), 257.

- [12] NAZEERUDDIN M.K., ZAKEERUDDIN S.M., HUMPHRY-BAKER R., JIROUSEK M., LISKA P., VLACHOPOULOS N., SHKLOVER V., FISCHER C.H., GRATZEL M., *Inorg. Chem.*, 38 (1999), 6298.
- [13] HARA K., DAN-OH Y., KASADA C., OHGA Y., SHINPO A., SUGA S., SAYAMA K., ARAKAWA H., *Langmuir*, 20 (2004), 4205.
- [14] RAMAKRISHNA G., VERMA S., JOSE D.A., KUMAR D.K., DAS A., PALIT D.K., GHOSH H.N., *J. Phys. Chem. B*, 110 (2006), 9012.
- [15] NAZEERUDDIN M.K., HUMPHRY-BAKER R., OFFICER D.L., CAMPBELL W.M., BURRELL A.K., GRATZEL M., *Langmuir*, 20 (2004), 6514.
- [16] SCHMIDT-MENDE L., CAMPBELL W.M., WANG Q., JOLLEY K.W., OFFICER D.L., NAZEERUDDIN M.K., GRATZEL M., *ChemPhysChem*, 6 (2005), 1253.
- [17] KOUMURA N., WANG Z.S., MORI S., MIYASHITA M., SUZUKI E., HARA K., *J. Am. Chem. Soc.*, 128 (2006), 14256.
- [18] KROEZE J.E., HIRATA N., KOOPS S., NAZEERUDDIN M.K., SCHMIDT-MENDE L., GRATZEL M., DURRANT J.R., *J. Am. Chem. Soc.*, 128 (2006), 16376.
- [19] MONTANARI I., NELSON J., DURRANT J.R., *J. Phys. Chem. B*, 106 (2002), 12203.
- [20] BESSHO T., ZAKEERUDDIN S.M., YEH C.Y., DIAU E.W.-G., GRATZEL M., *Angew. Chem. Int. Edit.*, 49 (2010), 6646.
- [21] YELLA A., LEE H.-W., TSAO H.N., YI C., CHANDIRAN A.K., NAZEERUDDIN M.K., DIAU E.W.-G., YEH C.-Y., ZAKEERUDDIN S.M., GRATZEL M., *Science*, 334 (2011), 629.
- [22] ZHAO Y., ZHAI J., TAN S.X., WANG L.F., JIANG L., ZHU D.B., *Nanotechnology*, 17 (2006), 2090.
- [23] ZHAO Y., CHEN W., ZHAI J., SHENG X.L., HE Q.G., WEI T.X., BAI F.L., JIANG L., ZHU D.B., *Chem. Phys. Lett.*, 445 (2007), 259.
- [24] ZABAN A., FERRERE S., SPRAGUE J., GREGG B.A., *J. Phys. Chem. B*, 101 (1997), 55.
- [25] RAMAKRISHNA G., SINGH A.K., PALIT D.K., GHOSH H.N., *J. Phys. Chem. B*, 108 (2004), 1701.
- [26] RAMAKRISHNA G., GHOSH H.N., SINGH A.K., PALIT D.K., MITTAL J.P., *J. Phys. Chem. B*, 105 (2001), 12786.
- [27] MOSER J.E., GRATZEL M., *Chem. Phys.*, 176 (1993), 493.
- [28] RAJH T., CHEN L.X., LUKAS K., LIU T., THURNAUER M.C., TIEDE D.M., *J. Phys. Chem. B*, 106 (2002), 10543.
- [29] HAGFELDT A., GRATZEL M., *Chem. Rev.*, 95 (1995), 49.

Received 2014-04-08

Accepted 2014-07-16